

## ADSORPTION PROPERTIES OF HYDROPHOBIC POROUS COORDINATION POLYMERS OF ZINC-OXALIC ACID WITH TRIAZOLE AND AMINO TRIAZOLE MIXTURE LIGANDS

Moondra Zubir<sup>1,2,✉</sup>, Zainuddin Muchtar<sup>1</sup>, Jasmidi Jasmidi<sup>1</sup>, Rini Selly<sup>1</sup>,  
Siti Rahmah<sup>1</sup>, Putri Faradilla<sup>1</sup>, Dikki Miswanda<sup>3</sup>

<https://doi.org/10.23939/chcht18.03.305>

**Abstract.** The porous coordination polymers were prepared from  $Zn^{2+}$  and oxalic acid with 2 linker ligands, 1,2,4-triazole (Taz) and 3-amino-1,2,4-triazole (ATaz). The adsorption of  $N_2$  after adsorption of degassed  $CO_2$  in the pore frameworks increased by 3 times. The flexibility of this structure is due to the interaction of  $CO_2$  molecules with the amine groups contained in it, thereby increasing its porosity.

**Keywords:** adsorption, porous coordination polymers, mixture ligands, triazole, amino triazole.

### 1. Introduction

Porous compounds have attracted the attention of chemists, physicists, and materials scientists due to their unique nature of nanometer space creation and adsorption. These compounds are also used in heterogeneous separation, storage, and catalysis<sup>1, 2</sup>. Recently, porous coordination polymers have been developed in addition to two other classes of porous materials such as inorganic materials (zeolites) and carbon-based materials.

The porous coordination polymers (PCPs) are composed of a central atom and a linker ligand to form a 3-dimensional structure that has special properties depending on the properties of the central atom and the binding ligand. PCPs were prepared for several applications, especially for gas storage, so they can be used to eliminate harmful gases in the environment<sup>3–6</sup>. Some PCPs have many properties as carbon dioxide gas capturers<sup>7–9</sup>, utilizing both the functional groups contained in ligands and the pore structure formed

by the formation of complexes with PCPs<sup>10</sup>. Some PCPs are also formed as flexible structures, with their skeletal structure changing as a result of absorption but not changing the pore structure of the PCPs<sup>11</sup>. This is also possible due to the presence of guest molecules in the pore structure, which are then replaced by gas molecules adsorbed during the physical adsorption process<sup>12–15</sup>.

When using a ligand containing an amino group, for example, aminotriazole (ATaz), no micropores appear during  $N_2$  adsorption, but  $CO_2$  can be adsorbed due to the reaction of amino groups ( $NH_2$ ) and  $CO_2$ <sup>16–19</sup>. Previously, we have prepared new PCP –  $[Zn_2(Oxac)(Taz)_2] \cdot (H_2O)_{2.5}$ , obtained from aqueous-methanol solutions of  $Zn_3(CO_3)_2(OH)_6$  and two types of ligands – oxalic acid (oxac) and 1,2,4-triazole (Taz). Oxalic acid was used as a co-ligand to form two-dimensional structures, as well as a linker to Taz and ATaz to form three-dimensional structures with high crystallinity. We have found a new way to form micropores during  $CO_2$  adsorption, which consists of filling the pores with water from the synthesis solvent. The adsorption of  $N_2$  on  $CO_2$  degassed after adsorption increases 5 times. The interaction of  $CO_2$  and  $H_2O$  molecules in the frameworks promotes the formation of micropores<sup>20, 21</sup>. There are limited reports on PCPs synthesis in which more than two kinds of ligands are used in one complex compound. The ratio of ligand interconnections and the proportional strength of the resulting coordination bonds become important for the incorporation of each ligand in the structure<sup>22, 23</sup>.

Porous coordination polymers prepared from  $Zn^{2+}$ , oxalic acid, and a mixture of 3-amino-1,2,4-triazole (ATaz) and 1,2,4-triazole (Taz) also were synthesized to promote the high adsorption amount of carbon dioxide. Molar fractions Taz / (Taz + ATaz) were prepared as 0.1; 0.3; 0.4; 0.5; 0.6; 0.7 and 0.9 and were compared with ATaz and Taz ligand<sup>21</sup>. The adsorption of nitrogen with a molar fraction of 0.5 has a high contribution to the largest surface area, which was calculated from the stage of pore cavity fusion and the existence of an amine group in the frameworks.

<sup>1</sup> Chemistry Department, Faculty of Mathematics and Natural Sciences, Universitas Negeri Medan, North Sumatera, Indonesia

<sup>2</sup> Chemistry Department, Faculty of Science, Shinshu University, Matsumoto, Nagano, Japan

<sup>3</sup> Mechanical Engineering Department, Politeknik Negeri Medan, Medan, North Sumatera, Indonesia

✉ moondrazubir@unimed.ac.id

© Zubir M., Muchtar Z., Jasmidi J., Selly R., Rahmah S., Faradilla P., Miswanda D., 2024

This phenomenon indicates that the combined effects of both ligands could produce a higher amount of carbon dioxide<sup>24</sup>.

In this study, we prepared PCPs using  $Zn^{2+}$  and oxalic acid with 1,2,4-triazole (Taz) without amine groups and 3-amino-1,2,4-triazole (ATaz) with amine groups as linker ligands. We also prepared a mixture of 1,2,4-triazole (Taz) and 1,2,4-triazole (Taz) with 0.3; 0.5 and 0.7 molar fractions of Taz / (Taz + ATaz). Nitrogen adsorption and  $CO_2$  adsorption were measured after  $CO_2$  degassing before  $CO_2$  adsorption without pretreatment. The flexibility of the structure due to the combination of the presence of water and carbon dioxide groups contained in the framework of the PCPs created higher  $CO_2$  molecules that could be adsorbed in these PCPs frameworks<sup>25–27</sup>.

## 2. Experimental

### 2.1. Materials

$Zn_5(CO_3)_2(OH)_6$  (Alfa Aesar, Co. Ltd.), oxalic acid (Wako Pure Chemical Industries, Ltd., WPCI), 1,2,4-triazole (WPCI), methanol (WPCI), and distilled water were used in this study.

### 2.2. Methods

#### 2.2.1. Porous Coordination Polymers (PCPs)

##### Synthesis

Zn-oxac-Taz ( $X = 1$ ) was prepared by the following procedure. 0.4 g of  $Zn_5(CO_3)_2(OH)_6$ , 0.4 g oxalic acid, and 1.4 g of 1,2,4-triazole/Taz were added to a mixed solvent of 12 mL of methanol and 2 mL of distilled water. The solution was transferred to a Teflon cell and put inside the autoclave vessel, then kept at a constant temperature of 453 K for 12 hours (Fig. 1).

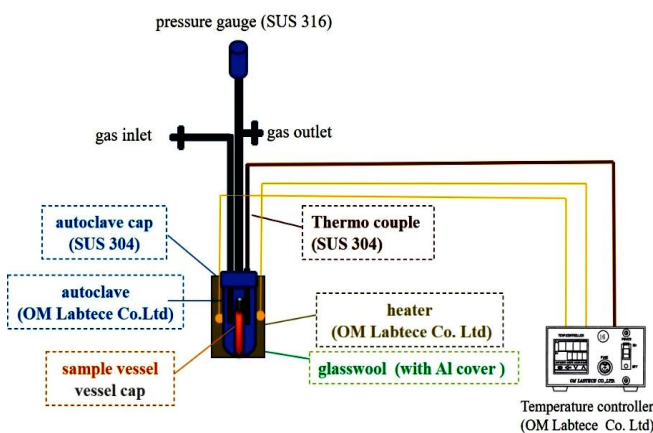


Fig. 1. Synthesis system of Zn-oxac-Taz/ATaz PCPs with various molar fraction

After 12 hours, the solution was cooled to room temperature, and the white precipitated crystals were filtered with a membrane filter. To obtain a pure crystal, the solution was washed with the solvent and dried in air at room temperature. An oxac-ATaz was prepared by the same procedure, the weight of oxalic acid was the same and  $Zn_5(CO_3)_2(OH)_6$  was mixed with 1.6 g of 3-amino-1,2,4-triazole (ATaz). The mixture ligands with 0.3 (30 % Taz and 70 % ATaz), 0.5 (50 % Taz and 50 % ATaz), and 0.7 (70 % Taz and 30% ATaz) molar fractions were prepared with the same amounts of  $Zn_5(CO_3)_2(OH)_6$  and oxalic acid as above.

#### 2.2.2. Porous Coordination Polymers (PCPs) Characterization

The prepared crystals of white color were analyzed by a Rigaku X-ray diffractometer (XRD) Multiflex with Cu-K $\alpha$  at 40 kV and 20 mA to determine the differences in the crystal structure of each PCP. The XRD pattern was determined by EXPO 2014<sup>24</sup> to investigate the crystal parameters of each PCP and the morphology was observed by using a JEOL scanning electron microscopy (SEM) JSM-7600 F.

#### 2.2.3. Adsorption Measurements

$N_2$  and  $CO_2$  adsorption were measured at 77 K and 303 K, respectively, by a custom-made volumetric adsorption system (Fig. 2). After each sample of ca. 100 mg was used for adsorption, then 3 kinds of adsorption treatments were used for  $N_2$  and  $CO_2$  adsorption measurements:

1. As a synthesized sample without pretreatment (0 h).
2. Pretreated at 333 K and 1 m Pa for 1 hour and then at 383 K for 12 hours.
3.  $CO_2$  adsorption. Degassing of the sample (1), and then continuing the second adsorption for  $N_2$  and  $CO_2$  adsorption.

Langmuir isotherm model was plotted to determine the surface area based on  $CO_2$  adsorption amount. The linear equation of the Langmuir isotherm model was placed in the equation below<sup>28</sup>:

$$\frac{C_e}{q_e} = \frac{1}{K_L q_m} + \frac{C_e}{q_m} \quad (1)$$

Langmuir surface area was determined from  $CO_2$  adsorption which used the Langmuir equation:

$$S_L = (q_m \cdot N_A \cdot a) / M, \quad (2)$$

where  $q$  is the number of  $CO_2$  molecules adsorbed at the monolayer of PCPs in  $mgg^{-1}$ ,  $N_A$  is Avogadro number;  $6.02 \cdot 10^{23} mol^{-1}$ ,  $a$  is an occupied surface area of one molecule of carbon dioxide (3.3 Å), and  $M$  is the molecular weight of carbon dioxide in  $gmol^{-1}$ <sup>29</sup>.

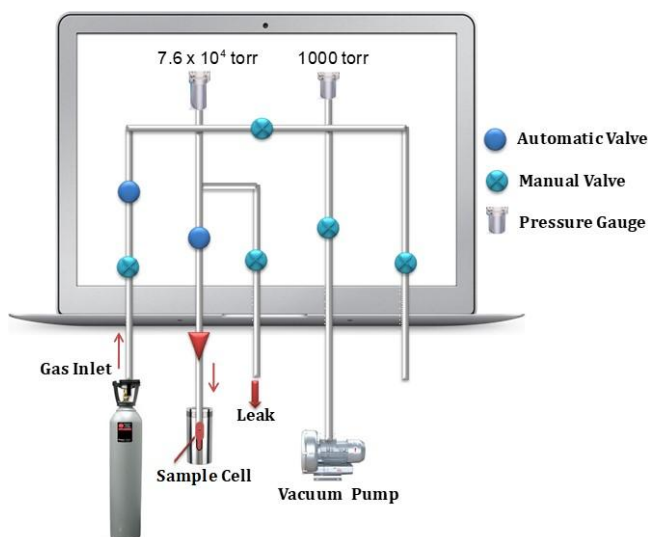


Fig. 2. Volumetric adsorption system of Zn-oxac-Taz/ATaz PCPs for Nitrogen and Carbon dioxide adsorption

### 3. Results and Discussion

#### 3.1. XRD and Structure Analysis of PCPs

Changes in the ratio of Taz to ATaz ligand were observed with changes in the crystal structure by XRD (Fig. 3). The composition of 30 % Taz and 70 % ATaz ( $X = 0.3$ ) induces a similar XRD pattern to Zn-oxac-ATaz ( $X = 0$ ), which contains only the ATaz ligand, although it shows a decrease in intensity on the PCP with  $X = 0.3$ . This is also indicated by the absence of changes in the crystal system for the PCPs with  $X = 0.3$  and  $X = 0$  (ATaz), which are formed as orthorhombic crystal systems (Table 1).

Similarly, Zn-oxac-Taz/ATaz with 70 % Taz or 30 % ATaz ( $X = 0.7$ ) also has a similar structure to Zn-oxac-Taz, which has only the Taz ligand, and the intensity of the main peak of Zn-oxac-Taz/ATaz ( $X = 0.7$ ) is also lower than Zn-oxac-Taz ( $X = 1$ ). Otherwise, the crystals of the system differ from each other in that Zn-oxac-Taz is monoclinic and Zn-oxac-Taz/ATaz ( $X = 0.7$ ) is triclinic. The difference in intensity on the XRD pattern leads to a slight change in the orientation of the crystal structure between these two crystals<sup>27</sup>. For Zn-oxac-Taz/ATaz with the same composition, significant structural changes between Taz and ATaz ligands were observed ( $X = 0.5$ ), indicating that the integration of 2 ligands with the same composition leads to the emergence of new properties due to the difference in the crystal system.

By using the Rietveld refinement derived from XRD pattern, crystal system constructed by the Vesta program<sup>30</sup>, depicts the crystal structure (without H<sub>2</sub>O) of the as-synthesized ZOTW<sub>2.5</sub>, having a five-coordinate

Zn<sup>2+</sup> ion connected to three Taz molecules and an oxalic acid (Fig. 4). The crystal has a 3-dimensional coordination network and micropores along the  $c$  axis, the size of which is estimated to be ca.  $0.30 \times 0.31 \times 0.40$  nm<sup>3</sup>. The composition and crystal structure were very similar to those of ZOATW<sub>0.5</sub> prepared by using ATaz instead of Taz, although its pore space may be filled with two solvent (water) molecules instead of two amino groups, as suggested by their compositions<sup>19, 20</sup>.

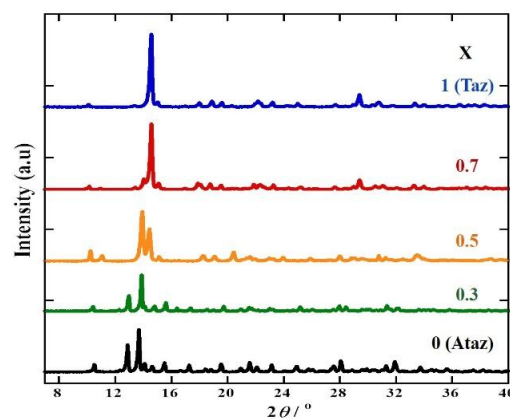


Fig. 3. XRD patterns of PCPs with different molar fractions, 0(ATaz); 0.3; 0.5; 0.7; and 1(Taz)

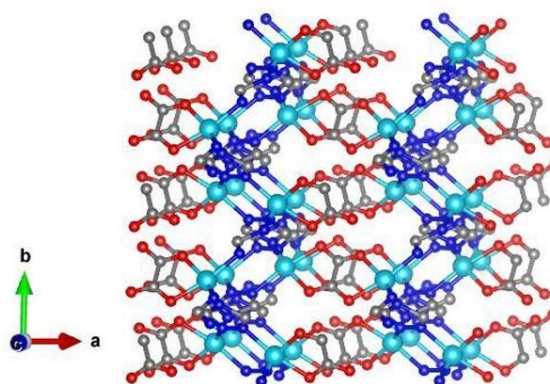


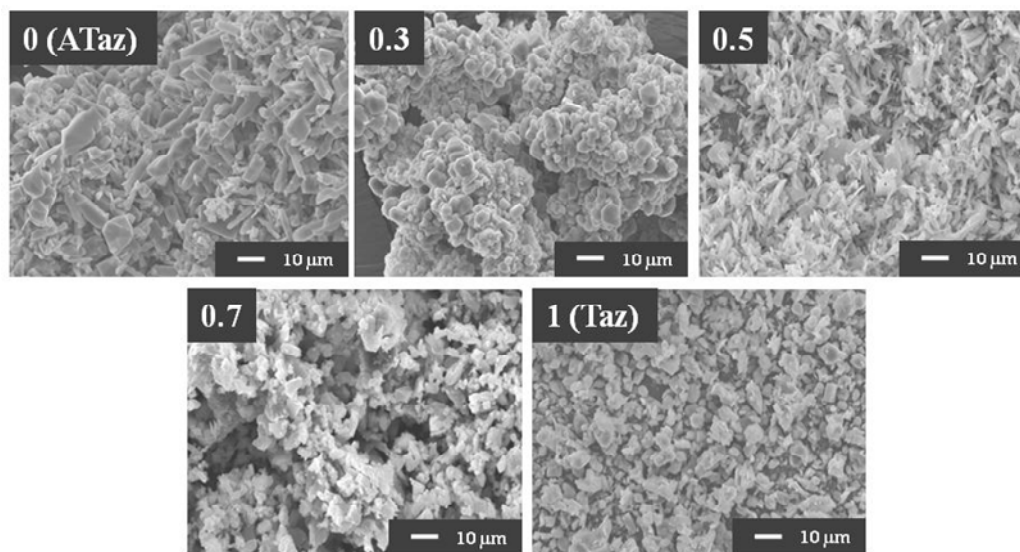
Fig. 4. Polymer structure of Zn atom (light blue) connected with oxalic acid (red) and triazole ligand (blue)

#### 3.2. SEM Image Observation

However, Zn-oxac-Taz/ATaz ( $X = 0.5$ ) induces a change in its crystal system to a triclinic system, which is similar to that of Zn-oxac-Taz/ATaz ( $X = 0.7$ ). To verify the homogeneity of the PCPs with this mixture of Taz and ATaz ligands, the crystal morphology was investigated by SEM. The SEM image (Fig. 5) shows that all the PCPs were homogeneous, indicating that the variations in the ratio of the Taz and ATaz ligand mixture could be formed properly, and the particle size of Zn-oxac-ATaz ( $X = 0$ ) appears larger than that of the other PCPs.

**Table 1.** Crystal parameters of PCPs with different molar fractions

PCPs Sample; X	A, Å	B, Å	C, Å	$\alpha$ , °	$\beta$ , °	$\gamma$ , °	V, Å <sup>3</sup>	Crystal System
Zn-oxac-ATaz; 0	13.74	16.82	12.94	90.00	90.00	90.00	2990.27	Orthorombic
Zn-oxac-Taz/ATaz; 0.3	13.66	16.98	12.77	90.00	90.00	90.00	2960.68	Orthorombic
Zn-oxac-Taz/ATaz; 0.5	10.71	10.56	9.97	104.97	109.14	103.97	960.44	Triclinic
Zn-oxac-Taz/ATaz; 0.7	13.75	9.13	8.89	90.48	103.71	106.69	1064.68	Triclinic
Zn-oxac-Taz; 1	10.03	7.97	9.34	90.00	110.66	90.00	986.18	Monoclinic

**Fig. 5.** SEM images of PCPs with various molar fraction, 0(ATaz); 0.3; 0.5; 0.7; and 1(Taz)

### 3.3. Nitrogen Adsorption Measurements

Nitrogen adsorption was carried out to observe the pore structure formed for all PCPs compounds (Fig. 6, A). Similar to the synthetic samples without pretreatment (both temperature and pressure), no induced pore changes were observed for Zn-oxac-ATaz ( $X = 0$ ), Zn-oxac-Taz ( $X = 1$ ), and Zn-oxac-Taz/ATaz ( $X = 0.3$ ). The presence of an amine group in the pores of Zn-oxac-ATaz ( $X = 0$ ) reduces the possibility of guest molecule penetration into the pores, indicating that the amine group blocks the pore space<sup>16</sup>. Whereas Zn-oxac-Taz ( $X = 1$ ) without pretreatment has little adsorbed N<sub>2</sub> at 77 K, indicating that the micropores are filled with water solvent, since the pore properties are hydrophobic<sup>21, 22</sup>. The presence of 30 % of the Taz group in Zn-oxac-Taz/ATaz ( $X = 0.3$ ) does not lead to the formation of open pores, as there are still 70 % of the ATaz groups inside the pores, which affect the ability of the N<sub>2</sub> molecule to be absorbed by the framework. However, if we determine the type of adsorption, it corresponds to type I, which indicates the formation of micropores.

Interestingly, Zn-oxac-Taz/ATaz ( $X = 0.5$ ) and Zn-oxac-Taz/ATaz ( $X = 0.7$ ) showed significant N<sub>2</sub> adsorption, confirmed by a saturation adsorption amount of ca.

85.15 mg/g and 144.98 mg/g, respectively. The presence of 50 % and 70 % of Taz ligand resulted in few solvents being trapped in the scaffolds due to the amine group of the ATaz ligand, as it is easier for the guest molecule to penetrate the scaffolds. The presence of the ATaz ligand, which is only 30 % in Zn-oxac-Taz/ATaz ( $X = 0.7$ ), also induces an increase in adsorption, as the pore space is free and suitable for filling with nitrogen molecules. The CO<sub>2</sub> adsorption isotherms were determined the same as for the synthetic samples without treatment (Fig. 6, B). Similarly to the N<sub>2</sub> adsorption results, Zn-oxac-ATaz ( $X = 0$ ) and Zn-oxac-Taz ( $X = 1$ ) did not show any adsorption, which supports the previous explanation due to the presence of amine groups in the pore of Zn-oxac-ATaz ( $X = 0$ ), as well as the presence of solvents in the hydrophobic pore of Zn-oxac-Taz ( $X = 1$ ). Zn-oxac-Taz/ATaz ( $X = 0.3$ ) and Zn-oxac-Taz/ATaz ( $X = 0.5$ ) PCPs showed optimal CO<sub>2</sub> absorption at 68.59 mg/g and 79.40 mg/g, respectively.

The presence of 50 % ATaz ligand of Zn-oxac-Taz/ATaz ( $X = 0.5$ ) and 70 % of ATaz ligand in Zn-oxac-Taz/ATaz ( $X = 0.3$ ) which is proportional to the number of amine groups contained in the frameworks creates a significant contribution to the number of CO<sub>2</sub> molecules adsorbed due to van der Waals interactions of the amine group with CO<sub>2</sub> molecules<sup>15, 20</sup>. The presence of the hy-

drophobic Taz ligand in the amount of 50 % in Zn-oxac-Taz/ATaz ( $X = 0.5$ ) and 30 % in Zn-oxac-Taz/ATaz ( $X = 0.3$ ) is not sufficient to block the penetration of  $\text{CO}_2$  molecules. Even the Taz ligands that do not belong to the amino group instead provide more space in the framework, and the presence of a small amount of solvent is likely to be blocked by the amino group originating from the ATaz ligand.

However, it is interesting that for Zn-oxac-Taz/ATaz ( $X = 0.7$ ), which contains 70 % Taz ligands, almost no  $\text{CO}_2$  was adsorbed at 300 torr at the initial stage, which may be due to the hydrophobic properties of the pores due to the presence of 70 % Taz ligands. This creates more solvent inside the pores compared to Zn-oxac-Taz/ATaz ( $X = 0.5$ ) and Zn-oxac-Taz/ATaz ( $X = 0.3$ ). However, at higher pressures above 300 torr,  $\text{CO}_2$  can gradually penetrate into the pores due to the

presence of 30 % ATaz ligands, which have an amine group capable of attracting  $\text{CO}_2$  in the amount of 120.43 mg/g. This gating pressure phenomenon can induce specific adsorption properties due to their flexible frameworks<sup>11,18</sup>.

To prove the presence of solvents due to the hydrophobic properties of the framework formed in the Taz ligand,  $\text{N}_2$  adsorption was also determined by pretreating the sample before the adsorption process (Fig. 7, A). The pretreatment was carried out at 333 K and 1 mPa for 1 hour, and then at 383 K for 12 hours. Zn-oxac-ATaz still shows no  $\text{N}_2$  uptake, which confirms the previous results if the pore framework was filled with an amine group rather than a solvent. The  $\text{N}_2$  uptake on Zn-oxac-Taz/ATaz ( $X = 0.3$ ) induced a slight increase compared to the previous treatment, from ca. 19.06 mg/g to 29.06 mg/g.

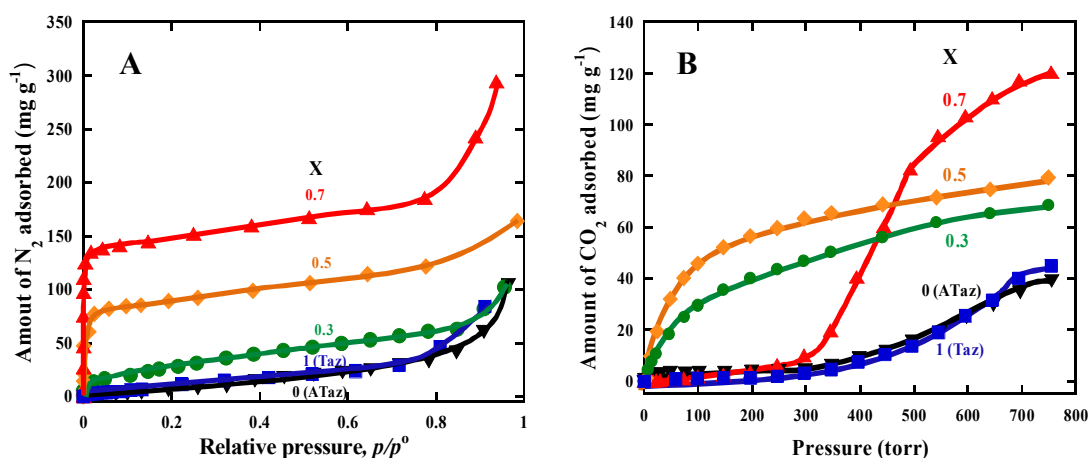


Fig. 6.  $\text{N}_2$  adsorption isotherms of as synthesized (PT; 0h) at 77 K (A) and  $\text{CO}_2$  adsorption isotherm at 303 K of all PCPs in various molar fraction (B)

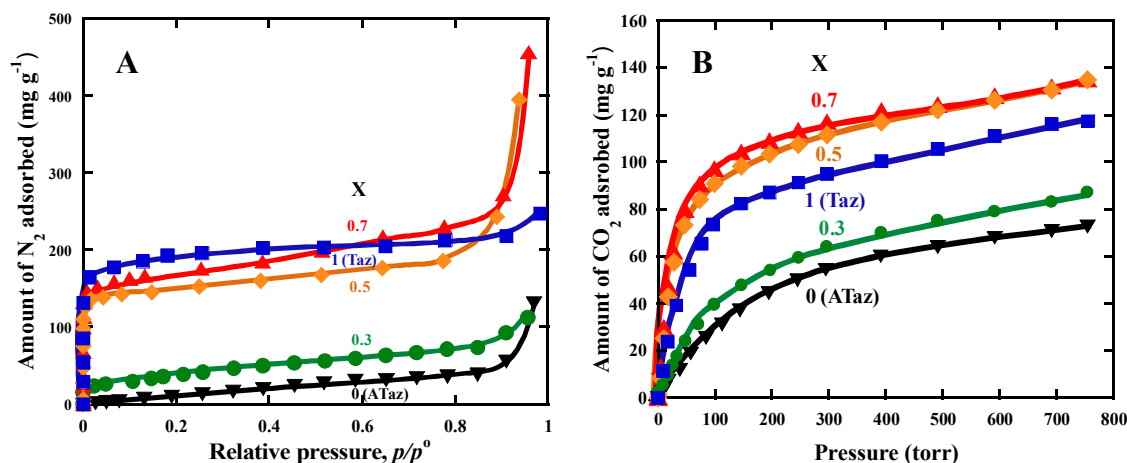


Fig. 7.  $\text{N}_2$  adsorption isotherms at 77 K (A) and  $\text{CO}_2$  adsorption isotherms at 303 K (B) of PCPs in various molar fraction after 12 h pretreatment

Similarly, Zn-oxac-Taz/ATaz ( $X = 0.5$ ) adsorbed  $N_2$  from 85.15 mg/g to 144.99 mg/g, and Zn-oxac-Taz/ATaz ( $X = 0.7$ ) adsorbed  $N_2$  from 144.98 mg/g to 162.67 mg/g. The release of solvents from the pores can be compared with the increase in the percentage of Taz-ligand in the PCP compounds. A larger number of micropores were formed after pretreatment for 12 hours. The highest  $N_2$  adsorption was observed for the Zn-oxac-Taz compound, indicating that all solvents left the pore skeleton to form micropores that showed adsorption at the saturation stage of 185.24 mg/g.

$CO_2$  adsorption was also determined after pretreatment at 333 K and 1 mPa for 1 hour and then at 383 K for 12 hours (Fig. 7, B). All PCPs adsorbed a significantly larger amount of  $CO_2$  compared to samples without pretreatment (Fig 7, B). Zn-oxac-Taz adsorbed up to 117.38 mg/g but Zn-oxac-Taz/ATaz ( $X = 0.5$ ) and Zn-oxac-Taz/ATaz ( $X = 0.7$ ) adsorbed higher amount of  $CO_2$ , 135.05 mg/g and 134.79 mg/g, respectively. Large open pores due to the release of solvents and the interaction of amine groups with  $CO_2$  molecules become the main factor in  $CO_2$  absorption in both PCPs, which increases the amount of  $CO_2$  absorbed compared to Zn-oxac-Taz ( $X = 1$ ).

The flexibility of Zn-oxac-Taz/ATaz ( $X = 0.7$ ) observed during  $CO_2$  adsorption without pretreatment (Fig.

7B) is confirmed by degassing after  $CO_2$  adsorption without pretreatment and continued adsorption of  $N_2$  and  $CO_2$ . A noticeable adsorption of  $N_2$  (Fig. 8, A) was observed due to the degassing process of  $CO_2$  molecules, which led to an induced expansion of the pore framework, confirming that all these PCPs are flexible. Zn-oxac-Taz ( $X = 0$ ), which previously did not exhibit micropore formation, formed type I micropores with a saturation adsorption value of about 149.18 mg/g. The increase in  $N_2$  uptake is proportional to the decrease in the content of amine groups in each of the PCPs. This is indicated by the highest  $N_2$  adsorption on Zn-oxac-Taz ( $X = 1$ ), which is 680.75 mg/g.

Regarding the reaction mechanism, amine attacks the  $CO_2$  carbon in the first step (Lewis base), producing in zwitterion  $RH_2N^+ - COO^-$ , or 1,3-zwitterion, where 1 and 3 stand for the positive and negative centers, respectively. Depending on the specific circumstances, the 1,3-zwitterion can either undergo an intramolecular hydrogen transfer to yield carbamic acid, or an intermolecular proton transfer with another amine (Bronsted base) to generate ammonium carbamate. When water combines with  $CO_2$ , it produces carbonic acid, which then reacts with amine to produce carbonate or bicarbonate. Water can also operate as a nucleophile. It might also release one amine molecule for further reaction with  $CO_2$  adsorption over amines<sup>31</sup>.

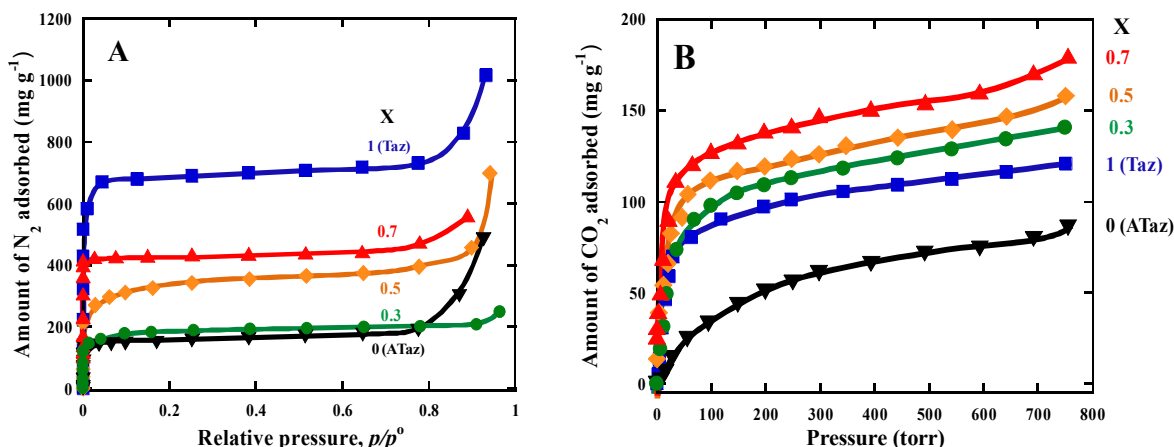


**Fig. 8.** Adsorption isotherms profile after degassed of  $CO_2$  adsorption (PT : 0h) and continue  $N_2$  adsorption at 77 K (A) and  $CO_2$  adsorption at 303 K (B) of PCPs in various molar fraction

The degassing process after  $CO_2$  adsorption without pretreatment is continued with  $CO_2$  adsorption. Zn-oxac-Taz/ATaz ( $X = 0.7$ ) showed the highest  $CO_2$  adsorption of 168.68 mg/g; Zn-oxac-Taz/ATaz ( $X = 0.5$ ) and Zn-oxac-Taz/ATaz ( $X = 0.3$ ) showed adsorption of 146.68 mg/g and 140.65 mg/g, respectively (Fig. 8, B). The size of the pore formed in Zn-oxac-Taz ( $X = 1$ ) contributed to a slight increase in  $CO_2$  uptake. The formation of micro-

pores and the presence of amine groups in Zn-oxac-Taz/ATaz with molar fractions of 0.3, 0.5 and 0.7 had a greater influence on  $CO_2$  adsorption. Zn-oxac-Taz/ATaz ( $X = 0.7$ ) can adsorb  $CO_2$  with the amounts of free pores due to the combination of the two effects. The action of 70 % Taz ligands, which provide sufficient space for  $CO_2$  penetration, is supported by 30 % ATaz ligands with amine groups, so the process of attracting a  $CO_2$

molecule by an amine group takes place together with sufficient space for penetrating the CO<sub>2</sub> molecules inside the pores.

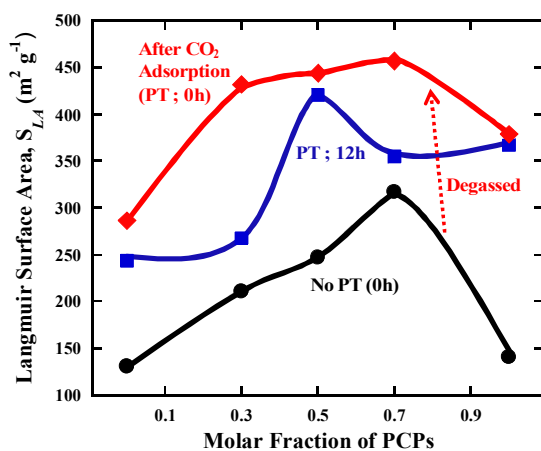


**Fig. 9.** Langmuir surface area of PCPs with different molar fractions without pretreatment (0 h), after 12 h of pretreatment and after degassed CO<sub>2</sub> adsorption (PT ; 0h)

Langmuir surface area was determined from CO<sub>2</sub> adsorption data under all conditions to observe the changes in the framework due to CO<sub>2</sub> degassing in order to explain the flexible properties of the structure of these five PCPs compounds (Fig. 9). During adsorption without pretreatment the surface area increases with an increase in percentage of Taz ligand in the pore. Zn-oxac-Taz ( $X = 1$ ) produces a small surface area of 180.86 m<sup>2</sup>g<sup>-1</sup> due to the pore filling with the solvent. The larger surface area of 317.07 m<sup>2</sup>g<sup>-1</sup> is produced by Zn-oxac-Taz/ATaz ( $X = 0.7$ ). After 12 hours of pretreatment, Zn-oxac-Taz/ATaz ( $X = 0.5$ ) produces the largest surface area of 420.78 m<sup>2</sup>g<sup>-1</sup>. The same composition of the Taz and ATaz ligands provides sufficient space for CO<sub>2</sub> to penetrate the framework after solvent removal, and the interaction of molecular CO<sub>2</sub> with amine groups contributes to a significant increase in adsorption. With this treatment, the surface area of all PCPs increased, indicating the presence of solvent that was trapped in the frameworks before the pretreatment changed the orientation of the crystals (crystal size and system). The flexibility of all PCPs was observed in the increase in surface area after CO<sub>2</sub> degassing and continued to the second adsorption without pretreatment. Zn-oxac-Taz/ATaz ( $X = 0.7$ ) has the largest surface area of 457.02 m<sup>2</sup>g<sup>-1</sup>.

## 4. Conclusions

The interaction of CO<sub>2</sub> with amine groups in the pore framework, which has slightly hydrophobic properties, produced remarkable effects for N<sub>2</sub> absorption. PCPs

contain 2 mixed ligand compositions of triazole (Taz), which does not contain an amine group, and aminotriazole (ATaz), which contains an amine group. N<sub>2</sub> adsorption with Zn-oxac-Taz ( $X = 1$ ) after degassed CO<sub>2</sub> adsorption gave a 3-fold increase from 185.24 mg/g to 680.75 mg/g, whereas PCPs from Zn-oxac-Taz/ATaz mixture ligands with  $X = 0.3$ ;  $X = 0.5$  and  $X = 0.7$  showed a doubled increase in surface area, and Zn-oxac-Taz/ATaz ( $X = 0.7$ ) produced the highest increase from 162.67 m<sup>2</sup>g<sup>-1</sup> to 431.17 m<sup>2</sup>g<sup>-1</sup>. The combined effect of empty space in the pore frameworks due to the presence of 70 % Taz ligand without amine group in the presence of 30 % ATaz ligand with amine group generated CO<sub>2</sub> adsorption after degassed CO<sub>2</sub> adsorption without pretreatment on Zn-oxac-Taz/ATaz ( $X = 0.7$ ), producing the largest adsorption amount of 168.68 mg/g. The flexibility of the structure due to the interaction of CO<sub>2</sub> molecules, water molecules (H<sub>2</sub>O) from the solvent, and amine groups contained in the frameworks increased CO<sub>2</sub> adsorption through the pretreatment process of the sample with temperature and pressure.

## References

- [1] Brostow, W.; Lobland, H.E.H.; Hamad, N.A. Dependence of Linear Isobaric Thermal Expansivity of Polymers on Their Flexibility. *Chem. Chem. Technol.* **2023**, *17*, 796–799. <https://doi.org/10.23939/chct17.04.796>
- [2] Kiöse, T.; Rakitskaya, T.; Ennan, A.; Vasylychko, V.; Gryshchouk, H. Composition and Activity of Copper-Palladium Catalyst on Carbon Fiber Material for Air Purification from Carbon Monoxide. *Chem. Chem. Technol.* **2024**, *17*, 272–278. <https://doi.org/10.23939/chct17.02.272>
- [3] Lin, L.C.; Kim, J.; Kong, Scott, X.E.; McDonald, T.M.; Long, J.R.; Reimer, J.A.; Smit, B. Understanding CO<sub>2</sub> Dynamics in Metal-Organic Frameworks with Open Metal Sites. *Angew. Chem., Int. Ed.* **2013**, *52*, 4410–4413. <https://doi.org/10.1002/anie.201300446>
- [4] Kitagawa, S.; Kitaura, R.; Noro, R. Functional Porous Coordination Polymers. *Angew. Chem. Int. Ed.* **2014**, *43*, 2334–2375. <https://doi.org/10.1002/anie.200300610>
- [5] Rosi, N.L.; Eckert, J.; Eddaoudi, M.; Vodak, D.T.; Kim, J.; O'keeffe, M.; Yaghi, O.M. Hydrogen Storage in Microporous Metal-Organic Frameworks. *Science* **2003**, *300*, 1127–1129. <https://doi.org/10.1126/science.1083440>
- [6] Onishi, S.; Ohmori, T.; Ohkubo, T.; Noguchi, H.; Di, L.; Hanzawa, Y.; Kanoh, H.; Kaneko, K. Hydrogen-Bond Change-Associated Gas Adsorption in Inorganic-Organic Hybrid Microporous Crystals. *Appl. Surf. Sci.* **2002**, *196*, 81–88. [https://doi.org/10.1016/S0169-4332\(02\)00048-X](https://doi.org/10.1016/S0169-4332(02)00048-X)
- [7] Millward, A.R.; Yaghi, O.M. Metal-Organic Frameworks with Exceptionally High Capacity for Storage of Carbon Dioxide at Room Temperature. *J. Am. Chem. Soc.* **2005**, *127*, 17998–17999. <https://doi.org/10.1021/ja0570032>
- [8] Garcia-Ricard, O.J.; Meza-Morales, P.; Silvia-Martinez, J.C.; Curet-Arana, M.C.; Hogan, J.A.; Hernandez-Maldonado, A.J. Carbon dioxide Storage and Sustained Delivery by Cu<sub>2</sub>(pzdc)<sub>2</sub>L [L = dipyrrolyl based ligand] Pillared-Layer Porous Coordination

- Networks. *Microporous Mesoporous Mater* **2013**, *177*, 54–58. <https://doi.org/10.1016/j.micromeso.2013.04.018>
- [9] Arstad B., Fjellvag H., Kongshaug K.O., Swang, O.; Blom, R. Amine Functionalised Metal Organic Frameworks (MOFs) as Adsorbents for Carbon Dioxide. *Adsorption*. **2008**, *14*, 755–762. <https://link.springer.com/article/10.1007/s10450-008-9137-6>
- [10] Kondo, M.; Yoshitomi, T.; Matsuzaka, H.; Kitagawa, S.; Seki K. Three-Dimensional Frameworks with Channeling Cavities for Small Molecules:  $\{[M_2(4,4'\text{-bpy})_3(\text{NO}_3)_4]\cdot x\text{H}_2\text{O}\}_n$  (M = Co, Ni, Zn). *Angew. Chem., Int. Ed. Engl.* **1997**, *36*, 1725–1777. <https://doi.org/10.1002/anie.199717251>
- [11] Eddaoudi, M.; Kim, J.; Rosi, N.L.; Vodak, D.; Wachter, J.; O’Keeffe, M.; Yaghi, O.M. Systematic Design of Pore Size and Functionality in Isoreticular MOFs and their Application in Methane Storage. *Science* **2002**, *295*, 469–472. <https://doi.org/10.1126/science.1067208>
- [12] Li, H.; Eddaoudi, M.; O’Keeffe, M.; Yaghi, O.M. Design and Synthesis of an Exceptionally Stable and Highly Porous Metal-Organic Framework. *Nature* **1999**, *402*, 276–279. <https://doi.org/10.1038/46248>
- [13] Garcia-Perez, P.; Serra-Crespo, P.; Hamad, S.; Kaptejin, F.; Gascon, J. Molecular Simulation of Gas Adsorption and Diffusion in a Breathing MOF Using a Rigid Force Field. *Phys.Chem.Chem.Phys.* **2014**, *16*, 16060–16066. <https://doi.org/10.1039/C3CP55416C>
- [14] Li, W.; Jia, H.P.; Ju, Z.F.; Zhang, J. Novel Chiral Cd(II) Coordination Polymer Based on Achiral Unsymmetrical 3-Amino-1,2,4-triazole with an Unprecedented  $\mu_4$ -Bridging Mode. *Cryst. Growth Des.* **2006**, *6*, 2136–2140. <https://doi.org/10.1021/cg060363w>
- [15] Soury, S.; Bahrami, A.; Alizadeh, S.; Shahna, F.G.; Nematollahi, D. Development of a Needle Trap Device Packed with HKUST-1 Sorbent for Sampling and Analysis of BTEX in Air. *Chem. Chem. Technol.* **2022**, *16*, 314–327. <https://doi.org/10.23939/chcht16.02.314>
- [16] Noro, S.; Kitagawa, S.; Akutagawa, T.; Nakamura, T. Coordination Polymers Constructed from Transition Metal Ions and Organic N-containing Heterocyclic Ligands: Crystal Structures and Microporous Properties. *Prog. Polym. Sci.* **2009**, *34*, 240–279. <https://doi.org/10.1016/j.proppolymsci.2008.09.002>
- [17] Li, J.R.; Ma, Y.; McCarthy, M.C.; Sculley, J.; Yu, J. Jeong, H.K.; Balbuena, P.B.; Zhou, H.C. Carbon Dioxide Capture-Related Gas Adsorption and Separation in Metal-Organic Frameworks. *Coord. Chem. Rev.* **2011**, *255*, 1791–1823. <https://doi.org/10.1016/j.ccr.2011.02.012>
- [18] Shimomura, S.; Horike, S.; Matsuda R.; Kitagawa, S. Guest Specific Function of a Flexible Undulating Channel in a 7,7,8,8-Tetracyano-p-quinodimethane Dimer-Based Porous Coordination Polymer. *J. Am. Chem. Soc.* **2007**, *129*, 10990–10991. <https://doi.org/10.1021/ja073505z>
- [19] Vaidhyanathan, R.; Iremonger, S.S.; Dawson, K.W.; Shimizu, G.K.H. An Amine-Functionalized Metal Organic Framework For preferential CO<sub>2</sub> Adsorption at Low Pressures. *Chem. Commun.* **2009**, 5230–5232. <https://doi.org/10.1039/B911481E>
- [20] Zubir, M.; Hamasaki, A.; Iiyama, T. Micropore Formation of  $[\text{Zn}_2(\text{Oxac})(\text{Taz})_2]\cdot(\text{H}_2\text{O})_{2.5}$  via CO<sub>2</sub> Adsorption. *Langmuir* **2017**, *33*, 680–684. <https://doi.org/10.1021/acs.langmuir.6b03456>
- [21] Zubir, M.; Hamasaki, A.; Iiyama, T. Magnetic Field Control of Micropore Formation in  $[\text{Zn}_2(\text{Oxac})(\text{Taz})_2]\cdot(\text{H}_2\text{O})_x$ . *Chem. Lett.* **2016**, *45*, 362–364. <https://doi.org/10.1246/cl.1511150>
- [22] Deng, H.; Doonan, C.J.; Furukawa, H.; Ferreira, R.B.; Towne, J.; Knobler, C.B.; Wang, B.; Yaghi, O.M. Multiple Functional Groups of Varying Ratios in Metal-Organic Frameworks. *Science* **2010**, *327*, 846–850. <https://doi.org/10.1126/science.1181761>
- [23] Cai, Y.; Zhang, Y.; Huang, Y.; Marder, S.R.; Walton, K.S. Impact of Alkyl-Functionalized BTC on Properties of Copper-Based Metal-Organic Frameworks. *Cryst. Growth Des.* **2012**, *12*, 3709–3713. <https://doi.org/10.1021/cg300518k>
- [24] Zubir, M.; Nasution, H.I.; Sudarma, T.F. The Role of Micropores and Amino Groups in Preferential CO<sub>2</sub> Adsorptivity of Porous Zn-Coordination Polymers Comprising Mixed Ligands of Triazole and Amino Triazole. *Orient. J. Chem.* **2019**, *35*, 449–454. <https://doi.org/10.13005/ojc/350158>
- [25] Couck, S.; Denayer, J.F.M.; Baron, G.V.; Remy, T.; Gascon, J.; Kaptejin, F. An Amine-Functionalized MIL-53 Metal-Organic Framework with Large Separation Power for CO<sub>2</sub> and CH<sub>4</sub>. *J. Am. Chem. Soc.* **2009**, *131*, 6326–6327. <https://doi.org/10.1021/ja900555r>
- [26] Banerjee, A.; Nandi, S.; Nasa, P.; Vaidhyanathan, R. Enhancing the Carbon Capture Capacities of a Rigid Ultra-Microporous MOF through Gate-Opening at Low CO<sub>2</sub> Pressures Assisted by Swiveling Oxalate Pillars. *Chem. Commun.* **2016**, *52*, 1851–1854. <https://doi.org/10.1039/C5CC08172F>
- [27] Zhai, Q.G.; Li, S.N.; Hu, M.C.; Jiang, Y.C. A Three-Dimensional Hybrid Framework Based on Novel  $[\text{Co}_4\text{Mo}_4]$  Bimetallic Oxide Clusters with 3,5-bis(3-Pyridyl)-1,2,4-triazole Ligands. *Acta Cryst.* **2009**, *C65*, m128–m130. <https://doi.org/10.1107/S0108270109003813>
- [28] Nguyen, K.D.; Tran, A.T.H.; Kaus, N.H.M. Preparation and Characterization of Red Mud-Based geopolymer Compositated with Rice Husk Ash for the Adsorption of Bromocresol Green in Aqueous Solution. *Chem. Chem. Technol.* **2023**, *17*, 857–869. <https://doi.org/10.23939/chcht17.04.857>
- [29] Itodo, A.U.; Itodo, H.U.; Gafar, M.K. Estimation of Specific Surface Area using Langmuir Isotherm Method. *J. Appl. Sci. Environ. Manage* **2011**, *14*, 141–145. <https://doi.org/10.4314/jasem.v14i4.63287>
- [30] Altomare, A.; Cuocci, C.; Giacobazzo, C.; Moliterni, A.; Rizzi, R.; Corriero, N.; Falcicchio, A. EXPO2013: A Kit of Tools for Phasing crystal Structures from Powder Data. *J. Appl. Crystallogr.* **2013**, *46*, 1231–1235. <https://doi.org/10.1107/S0021889813013113>
- [31] Said, R.B.; Kolle, J.M.; Essalah, K.; Tangour, B.; Sayari, A. A Unified Approach to CO<sub>2</sub>-Amine Reaction Mechanisms. *ACS Omega* **2020**, *5*, 26125–26133. <https://doi.org/10.1021/acsomega.0c03727>

Received: March 14, 2024 / Revised: April 23, 2024 / Accepted: July 03, 2024

## АДСОРБЦІЙНІ ВЛАСТИВОСТІ ГІДРОФОБНИХ ПОРИСТИХ КООРДИНАЦІЙНИХ ПОЛІМЕРІВ ЦИНК-ОКСАЛАТНОЇ КИСЛОТИ З ЛІГАНДАМИ СУМІШІ ТРИАЗОЛУ Й АМІНОТРИАЗОЛУ

**Анотація.** Пористі координаційні полімери одержано з  $\text{Zn}^{2+}$  та оксалатної кислоти з двома лінкерними лігандами – 1,2,4-триазолом (Taz) та 3-аміно-1,2,4-триазолом (ATaz). Адсорбція  $\text{N}_2$  після адсорбції дегазованого  $\text{CO}_2$  в пористій структурі зростає утричі. Гнучкість цієї структури зумовлена взаємодією молекул  $\text{CO}_2$  з аминними групами, що містяться в ній, завдяки чому збільшується її пористість.

**Ключові слова:** адсорбція, пористі координаційні полімери, змішані ліганди, триазол, амінотриазол.